

# Database of 3D Grid-Based Numerical Breast Phantoms for use in Computational Electromagnetics Simulations

E. Zastrow, S. K. Davis, M. Lazebnik, F. Kelcz, B. D. Van Veen, and S. C. Hagness

Department of Electrical and Computer Engineering  
University of Wisconsin-Madison

## Repository overview

This online repository provides a database of anatomically realistic numerical breast phantoms that can be used in computational electromagnetics simulations based on methods such as the finite-difference time-domain (FDTD) method [1]. The phantoms capture the structural heterogeneity of normal breast tissue and incorporate the realistic dispersive dielectric properties of normal breast tissue from 0.5 to 20 GHz reported by Lazebnik et al [2], [3].

The breast phantoms are derived from series of T1-weighted magnetic resonance images (MRIs) of patients in a prone position. Each phantom is comprised of a 3D grid of cubic voxels, where each voxel is 0.5mm x 0.5mm x 0.5mm. The breast model includes a roughly 1.5-mm-thick skin layer, a 1.5-cm-thick subcutaneous fat layer at the base of the breast, and a 0.5-cm-thick muscle chest wall.

We believe that these phantoms will be of use to the bioelectromagnetics research community and are providing them free of charge. We kindly ask that you reference the online repository and acknowledge the authors at the University of Wisconsin-Madison in any publication that is derived from the use of these phantoms.

## Repository files

Three ASCII text files are provided for each phantom. Below, the contents of each file are described in detail.

---

The first file, *breastInfo.txt*, gives the following basic information about the phantom: an internal (UW) identifier number [“breast ID”], dimensions of the grid in units of grid cells [“s1”, “s2”, “s3”], and the classification of breast composition [“classification”]. The numerical phantoms are classified according to their radiographic density, defined by the American College of Radiology [4], as follows: almost entirely fat (<25% glandular tissue), scattered fibroglandular tissue (25-50% glandular), heterogeneously dense breast (51-75% glandular), and very dense breast (>75% glandular). These tissue density classes are coded as 1, 2, 3, and 4, respectively, in the “classification” field.

An example of the contents of *breastInfo.txt*:

```
breast ID=012204
s1=316
s2=352
s3=307
classification=2
```

---

The second file, *mtype.txt*, provides tissue type information for each voxel in the grid. The file contains a single column of data, with each row representing a different voxel in the grid. The data file was generated using the following ordering of grid cells:

```

for kk=1:s3
  for jj=1:s2
    for ii=1:s1
      fprintf(fid, '%1.1f\n', ARRAY(ii, jj, kk));
    end
  end
end

```

where the dimension of **ARRAY** is [s1 x s2 x s3]

Each row contains one of the media numbers given in Table 1. The immersion medium media number is assigned to all voxels outside of the breast. The muscle media number is assigned to all voxels in the chest wall region. Media numbers associated with normal breast tissue are assigned to all voxels within the breast interior and the subcutaneous fat layer at the base of the breast. We categorize the normal breast tissue in the breast phantom into seven tissue types, ranging from the highest-water-content fibroconnective/glandular tissue with the highest dielectric properties (media number = 1.1), to the lowest-water-content fatty tissue with the lowest dielectric properties (media number = 3.3). There is also a transitional region (media number = 2) with intermediate dielectric properties. Figure 1 shows the spatial distribution of media numbers in a sagittal slice provided in *mtype.txt*.

| Tissue type                 | Media number |
|-----------------------------|--------------|
| Immersion medium            | -1           |
| Skin                        | -2           |
| Muscle                      | -4           |
| Fibroconnective/glandular-1 | 1.1          |
| Fibroconnective/glandular-2 | 1.2          |
| Fibroconnective/glandular-3 | 1.3          |
| Transitional                | 2            |
| Fatty-1                     | 3.1          |
| Fatty-2                     | 3.2          |
| Fatty-3                     | 3.3          |

**Table 1.** Tissue types and corresponding media numbers.

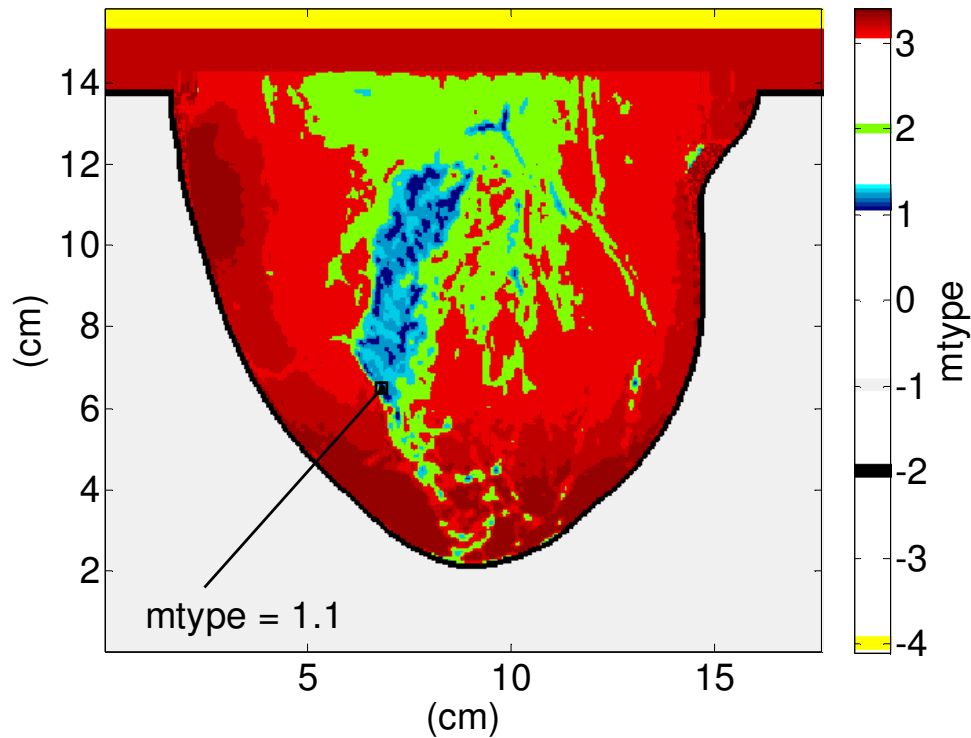


**Figure 1.** Example of the spatial distribution of media numbers (provided in *mtype.txt*) in a sagittal slice from a 3D numerical breast phantom (breast ID: 012204).

---

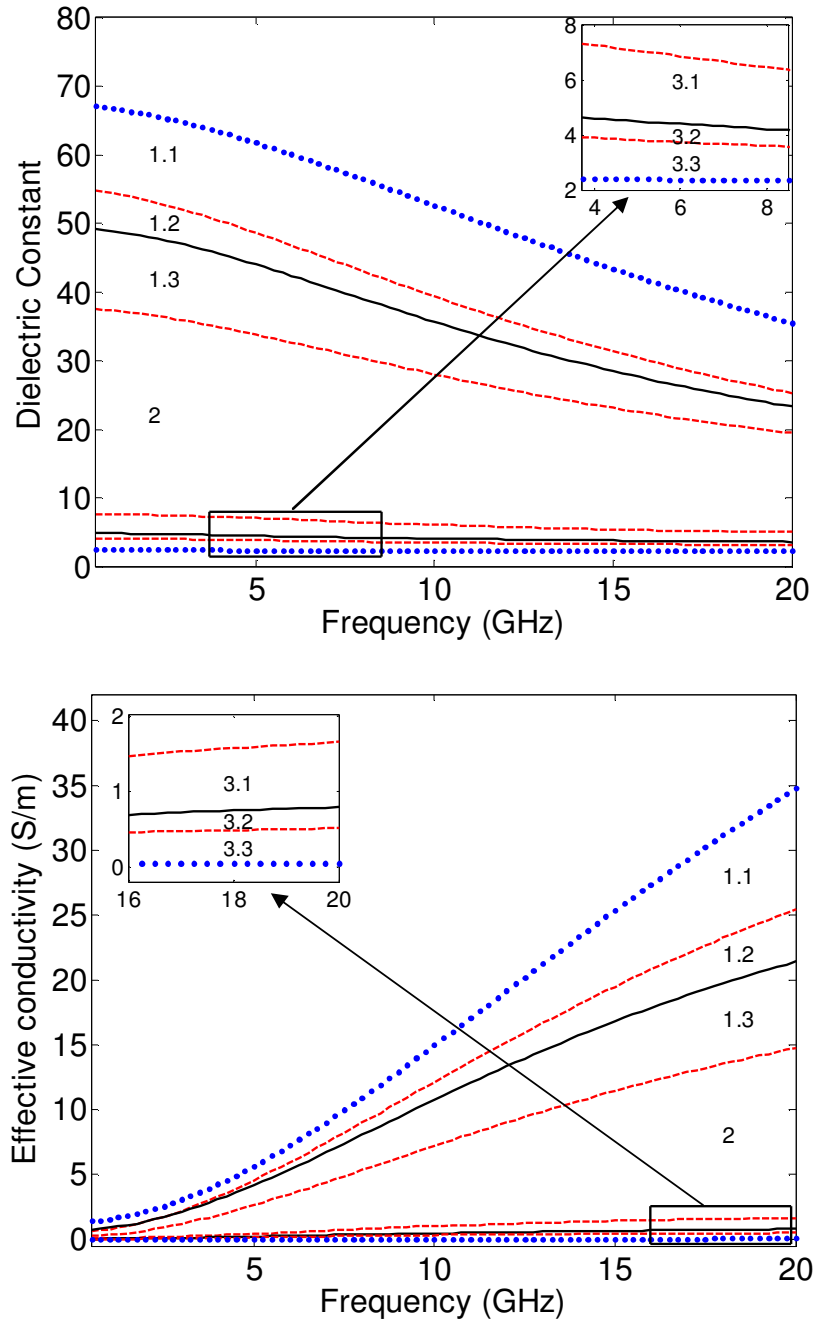
The third file, *pval.txt*, gives dielectric properties information for each voxel of the breast interior. Before we describe how to use the contents of this file, we provide some background material on the dielectric properties of normal breast tissue. We strongly encourage the user to read [2] before proceeding.

Figure 2 shows the eight wideband dielectric properties curves that serve as upper and lower bounds on each of the seven types of normal breast tissue listed in Table 1 from 0.5 to 20 GHz. The bold-faced numbers in Figure 2 correspond to the media numbers defined in Table 1.

- The maximum and minimum curves (shown as dotted **blue curves**) are the overall upper and lower bounds, respectively, on the frequency-dependent dielectric properties data presented in [2]. The lower blue dotted curve corresponds to the dielectric properties of lipids measured in our laboratory, while the upper blue dotted curve corresponds to the frequency-by-frequency maximum dielectric properties (envelope) of all the curves shown in Figure 8 in [2].
- The solid **black curves** are the median dielectric properties curves associated with the adipose-defined tissue group 1 and 3 reported in [2]. We refer to the two curves as “group1-median” and “group3-median” curves.
- The two pairs of dashed **red curves** are the 25<sup>th</sup> and 75<sup>th</sup> percentile dielectric properties curves associated with the adipose-defined tissue groups 1 and 3. We refer to the curves

as “group1-low” (25<sup>th</sup> percentile, group 1), “group1-high” (75<sup>th</sup> percentile, group 1), “group3-low” (25<sup>th</sup> percentile, group 3), and “group 3-high” (75<sup>th</sup> percentile, group 3).

The single-pole Cole-Cole parameters for the maximum, group1-high, group1-median, group1-low, group3-high, group3-median, group3-low, and minimum curves are summarized in Table 2.



**Figure 2.** The dielectric properties of normal breast tissue. The seven tissue-type regions bounded by the curves in this graph are labeled with the media numbers reported in Table 1. From top to bottom, the curves correspond to the following eight cases: maximum, group1-high, group1-median, group1-low, group3-high, group3-median, group3-low, and minimum.

|                      | $\epsilon_{\infty}$ | $\Delta\epsilon$ | $\tau$ (ps) | $\alpha$ | $\sigma_s$ (S/m) |
|----------------------|---------------------|------------------|-------------|----------|------------------|
| <b>minimum</b>       | 2.293               | 0.141            | 16.40       | 0.251    | 0.002            |
| <b>group3-low</b>    | 2.908               | 1.200            | 16.88       | 0.069    | 0.020            |
| <b>group3-median</b> | 3.140               | 1.708            | 14.65       | 0.061    | 0.036            |
| <b>group3-high</b>   | 4.031               | 3.654            | 14.12       | 0.055    | 0.083            |
| <b>group1-low</b>    | 9.941               | 26.60            | 10.90       | 0.003    | 0.462            |
| <b>group1-median</b> | 7.821               | 41.48            | 10.66       | 0.047    | 0.713            |
| <b>group1-high</b>   | 6.151               | 48.26            | 10.26       | 0.049    | 0.809            |
| <b>maximum</b>       | 1.000               | 66.31            | 7.585       | 0.063    | 1.370            |

**Table 2.** Single-pole Cole-Cole parameters for the dielectric properties associated with maximum, group1-high, group1-median, group1-low, group3-high, group3-median, group3-low, and minimum curves shown in Figure 2.

The format of *pval.txt* is also single column, and was generated using the same voxel ordering as *mtype.txt*.

In *pval.txt*, each voxel that represents normal breast tissue or subcutaneous fat has a value of  $p$  within the range [0,1], where lower values of  $p$  correspond to lower dielectric properties values within the given tissue type and higher values of  $p$  correspond to higher dielectric properties values. The values of  $p$  for all other voxels are set to zero. Figure 3 shows the spatial distribution of the values of  $p$  for the same sagittal slice through the 3D numerical breast phantom shown Figure 1.

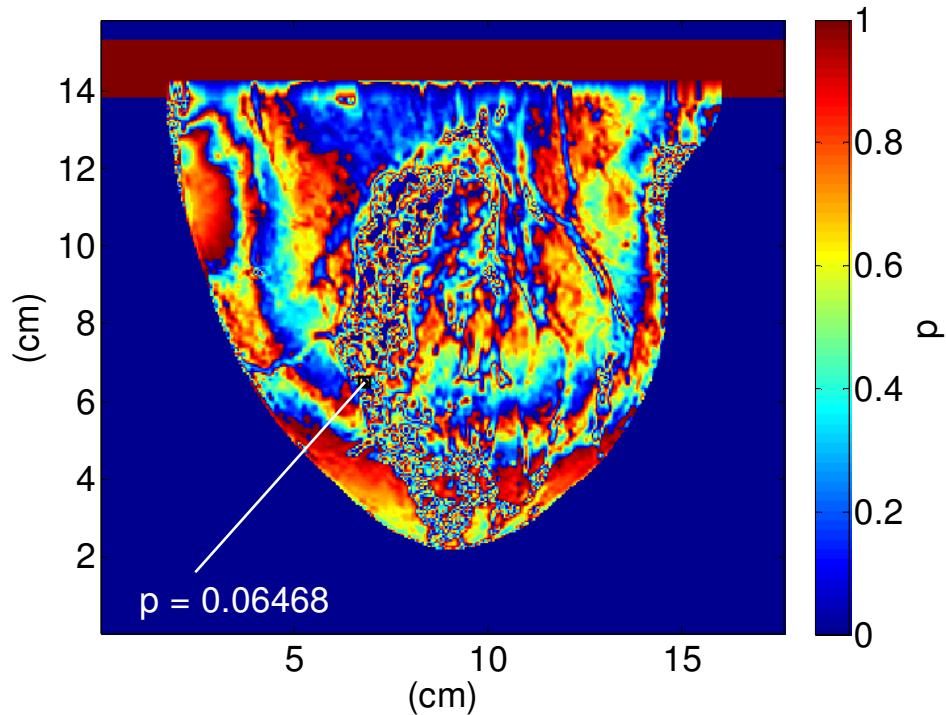


**Figure 3.** Example of the spatial distribution of  $p$  (provided in *pval.txt*) in a sagittal slice from a 3D numerical breast phantom (breast ID: 012204).

---

### File utilization

In this section we illustrate how to use the information provided by *mtype.txt* and *pval.txt*. Consider the specific voxel marked by the arrows in Figures 1 and 3 for the phantom with breast ID = 012204. The file *mtype.txt* indicates that the selected voxel has a media number of 1.1, which corresponds to the fibroconnective/glandular-1 tissue type (see Table 1). The file *pval.txt* indicates that the value of  $p$  for the selected voxel is  $p = 0.06468$ . As shown in Figure 4, the dielectric properties values associated with the fibroconnective/glandular-1 tissue type ( $mtype = 1.1$ ) fall in the region bounded from above by the maximum curve and from below by the group1-high curve (highlighted in red). Let  $cc\_upper$  be equal to the dielectric constant (or conductivity) value of the maximum curve at a specific frequency  $f$ , and let  $cc\_lower$  be equal to the dielectric constant (or conductivity) value of the group1-high curve at that same frequency.

The user can now compute the frequency-dependent dielectric properties from 500 MHz to 20 GHz as a weighted average of the data from the upper- and lower-bound curves as follows:

$$cc\_selected = p*cc\_upper + (1-p)*cc\_lower$$

This results in the blue dotted line in Figure 4 for the specific voxel in this illustration. This process can be repeated to obtain the frequency-dependent dielectric properties assigned to every voxel in the breast interior. Figure 5 shows the dielectric properties at 6 GHz, determined in the manner described here, for the phantom with breast ID = 012204

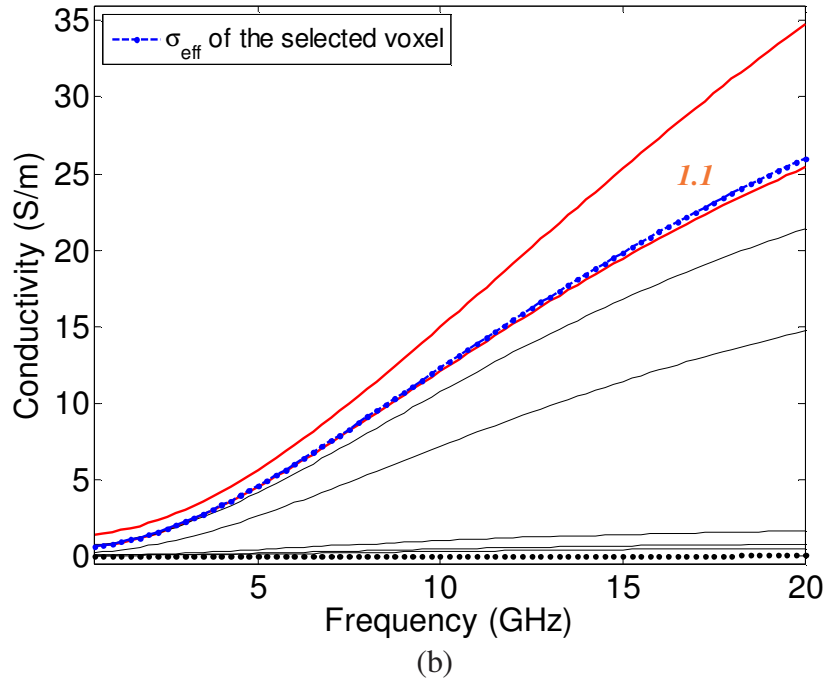
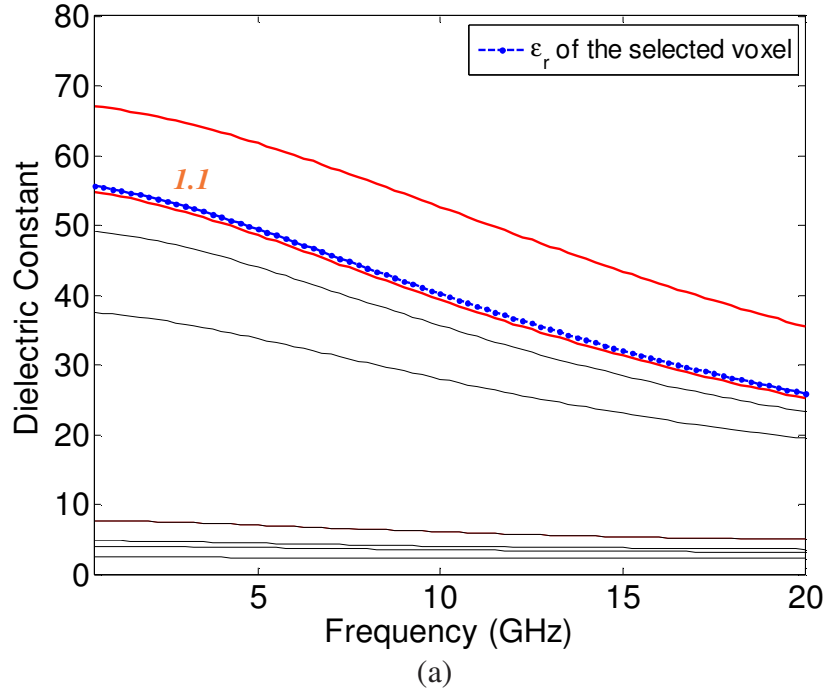
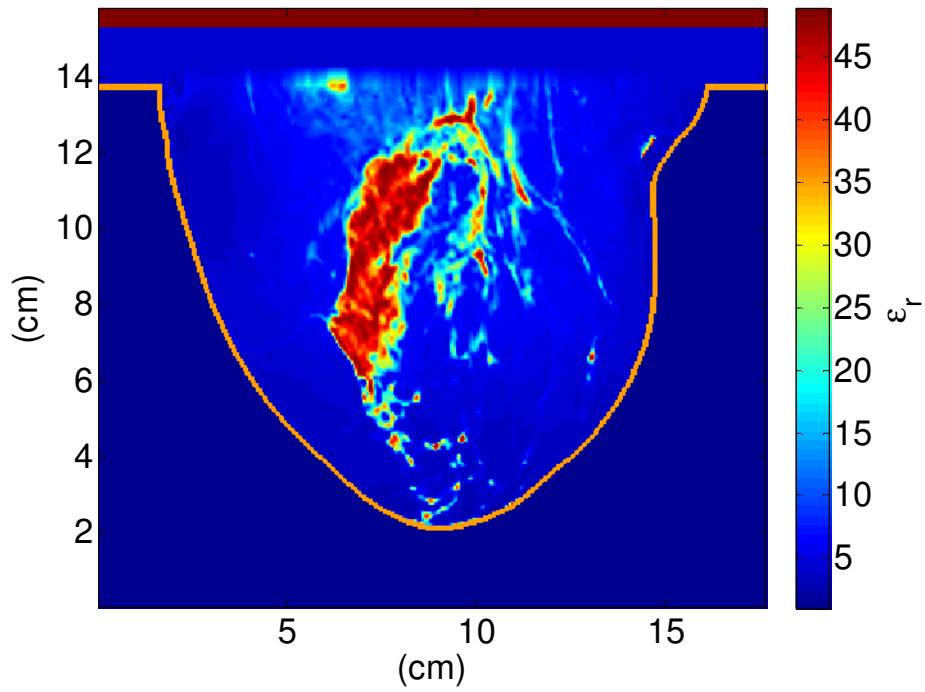
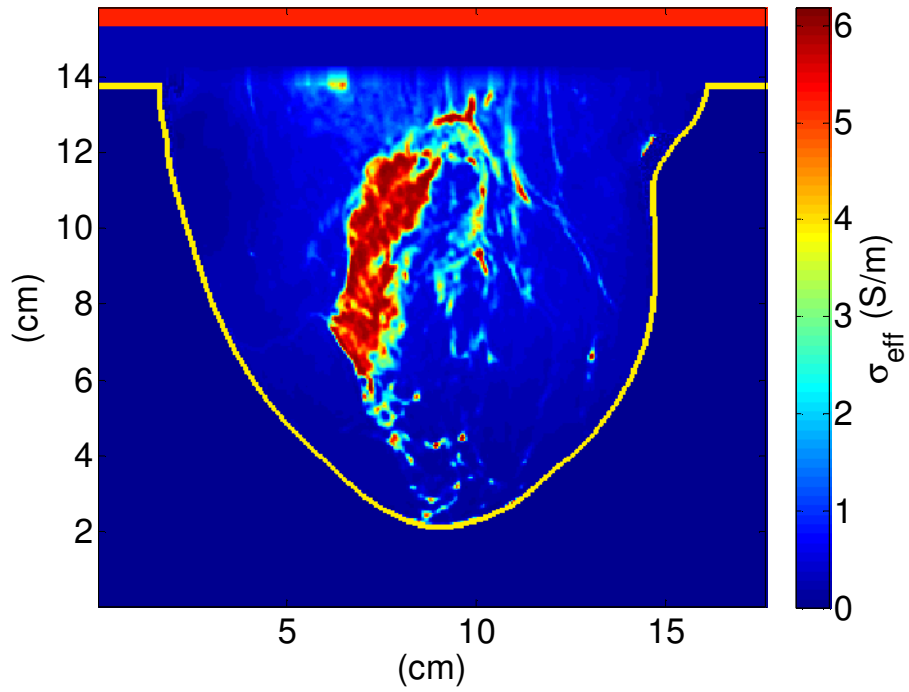


**Figure 4.** Frequency-dependent dielectric properties of a selected voxel with  $mtype = 1.1$  and  $p = 0.06468$ . (a) Dielectric constant. (b) Effective conductivity.



(a)



(b)

**Figure 5.** Example of the spatial distribution of the dielectric properties at 6 GHz in a sagittal slice from a 3D numerical breast phantom (breast ID = 012204). (a) Dielectric constant. (b) Effective conductivity (S/m).



---

### Conversion to Debye parameters

The frequency dependence of tissue dielectric properties is more readily incorporated into wideband FDTD simulations using Debye dispersion parameters rather than Cole-Cole parameters [5]. Lazebnik et al [5] reported one- and two-pole Debye models that retain the high accuracy of the Cole-Cole models for the dispersive dielectric properties of breast tissue. Model parameters were derived for two sets of frequency ranges: the entire measurement frequency range from 0.5 to 20 GHz, and the 3.1-10.6 GHz FCC band allocated for ultrawideband medical applications.

Here, in Table 3, we provide the parameters for single-pole Debye models that achieve excellent fits to the single-pole Cole-Cole models summarized in Table 2 over the 3-10 GHz band. These parameters differ slightly from those reported in [5] because here  $\tau$  is fixed for all tissue types<sup>1</sup> and only  $(\epsilon_\infty, \Delta\epsilon, \sigma_s)$  are allowed to vary in the fitting process. For skin and muscle tissues, we fit single-pole Debye models to the four-pole Cole-Cole models reported in [6] over the same frequency range. The single-pole Debye curves for normal breast tissue are shown in Figure 6 along with their corresponding Cole-Cole curves, to illustrate the accuracy of the Debye models over the 3-10 GHz band. Debye parameters for specific voxels in the breast interior can be computed using a weighted average based on the p value of a specific voxel (as described in the “File utilization” section above); note, however, that the weighted averages are applied to the Debye parameters themselves rather than the frequency-specific dielectric constant and conductivity.

|                      | $\epsilon_\infty$ | $\Delta\epsilon$ | $\tau$ (ps) | $\sigma_s$ (S/m) |
|----------------------|-------------------|------------------|-------------|------------------|
| <b>minimum</b>       | 2.309             | 0.092            | 13.00       | 0.005            |
| <b>group3-low</b>    | 2.848             | 1.104            | 13.00       | 0.005            |
| <b>group3-median</b> | 3.116             | 1.592            | 13.00       | 0.050            |
| <b>group3-high</b>   | 3.987             | 3.545            | 13.00       | 0.080            |
| <b>group1-low</b>    | 12.99             | 24.40            | 13.00       | 0.397            |
| <b>group1-median</b> | 13.81             | 35.55            | 13.00       | 0.738            |
| <b>group1-high</b>   | 14.20             | 40.49            | 13.00       | 0.824            |
| <b>maximum</b>       | 23.20             | 46.05            | 13.00       | 1.306            |
| <b>skin</b>          | 15.93             | 23.83            | 13.00       | 0.831            |
| <b>muscle</b>        | 21.66             | 33.24            | 13.00       | 0.886            |

**Table 3.** Single-pole Debye parameters for the maximum, group1-high, group1-median, group1-low, group3-high, group3-median, group3-low, and minimum curves associated with normal breast tissue as well as skin and muscle (valid for the 3 – 10 GHz band).

---

<sup>1</sup> The use of a constant relaxation time constant for all tissue types permits weighted averages to be employed in the generation of Debye parameters for each voxel in the computational grid.

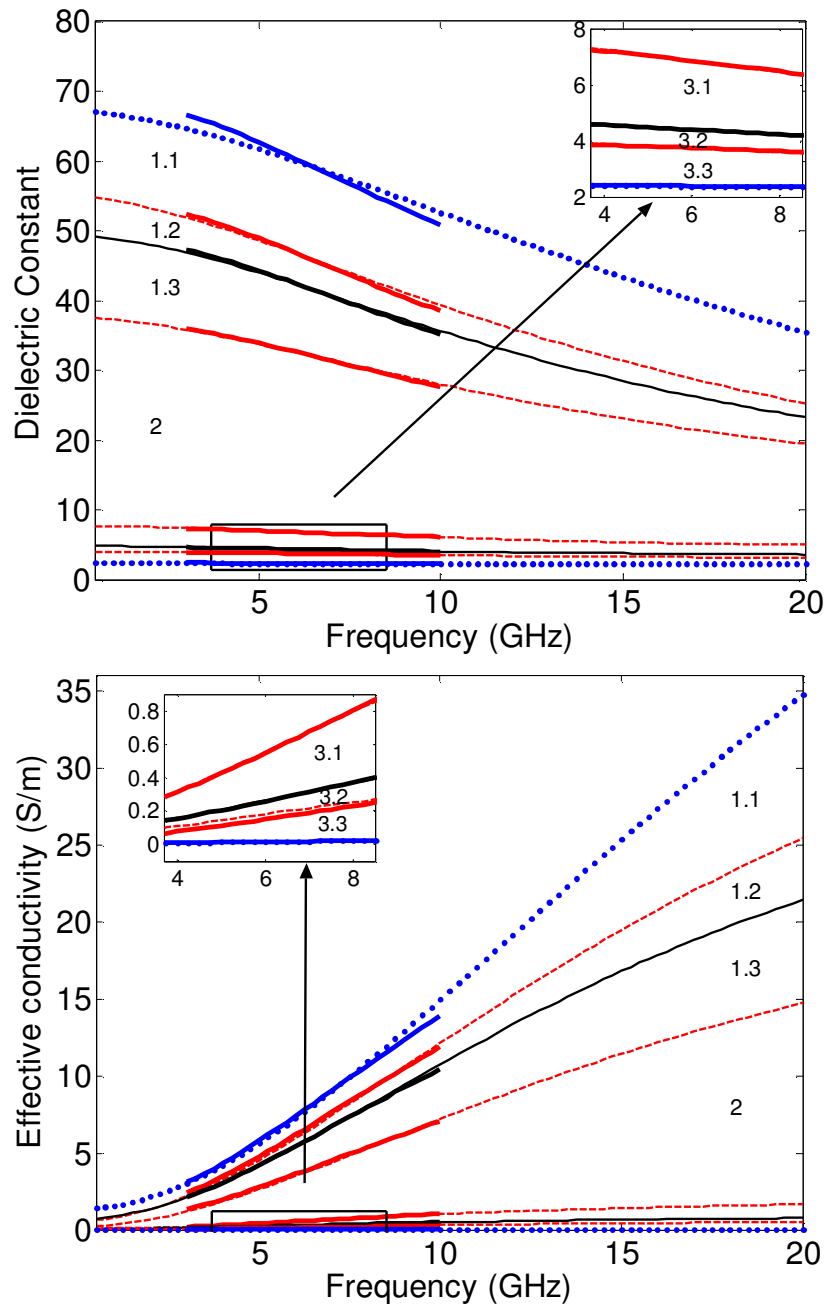


**Figure 6.** From top to bottom, the Cole-Cole and Debye (**bold**) curves correspond to the following eight cases: maximum, group1-high, group1-median, group1-low, group3-high, group3-median, group3-low, and minimum.

## References

- [1] A. Taflove and S. C. Hagness, *Computational Electrodynamics: The Finite-Difference Time-Domain Method*, 3<sup>rd</sup> ed., 2005.
- [2] M. Lazebnik, L. McCartney, D. Popovic, C. B. Watkins, M. J. Lindstrom, J. Harter, S. Sewall, A. Magliocco, J. H. Booske, M. Okoniewski, and S. C. Hagness, "A large-scale study of the ultrawideband microwave dielectric properties of normal breast tissue obtained from reduction surgeries," *Physics in Medicine and Biology*, vol. 52, pp. 2637-2656, April 2007.
- [3] M. Lazebnik, D. Popovic, L. McCartney, C. B. Watkins, M. J. Lindstrom, J. Harter, S. Sewall, T. Ogilvie, A. Magliocco, T. M. Breslin, W. Temple, D. Mew, J. H. Booske, M. Okoniewski, and S. C. Hagness, "A large-scale study of the ultrawideband microwave dielectric properties of normal, benign, and malignant breast tissues obtained from cancer surgeries," *Physics in Medicine and Biology*, in press.
- [4] American College of Radiology, *Breast Imaging Reporting and Data System (BI-RADS®)*, 4<sup>th</sup> ed., 2003.
- [5] M. Lazebnik, M. Okoniewski, J. H. Booske, and S. C. Hagness, "Highly accurate Debye models for normal and malignant breast tissue dielectric properties at microwave frequencies," *IEEE Microwave and Wireless Components Letters*, Dec. 2007, in press.
- [6] S. Gabriel, R. W. Lau, and C. Gabriel, "The dielectric properties of biological tissues: III. Parametric models for the dielectric spectrum of tissues," *Physics in Medicine and Biology*, vol. 41, pp. 2271-2293, 1996.